Journal of the Microelectronics & Packaging Society
Vol. 21, No. 1, p. 13-17. 2014
http://dx.doi.org/10.6117/kmeps.2014.21.1.013

Compositional Study of Surface, Film, and Interface of Photoresist-Free Patternable SnO_2 Thin Film on Si Substrate Prepared by Photochemical Metal-Organic Deposition

Yong-June Choi, Kyung-Mun Kang and Hyung-Ho Park†

Department of Materials Science and Engineering, Yonsei University, 50 Yonsei-ro, Seodaemun-gu, Seoul 120-749, Korea

(Received March 7, 2014: Corrected March 18, 2014: Accepted March 26, 2014)

Abstract: The direct-patternable SnO_2 thin film was successfully fabricated by photochemical metal-organic deposition. The composition and chemical bonding state of SnO_2 thin film were analyzed by using X-ray photoelectron spectroscopy (XPS) from the surface to the interface with Si substrate. XPS depth profiling analysis allowed the determination of the atomic composition in SnO_2 film as a function of depth through the evolution of four elements of C 1s, Si 2p, Sn 3d, and O 1s core level peaks. At the top surface, nearly stoichiometric SnO_2 composition (O/Sn ratio is 1.92.) was observed due to surface oxidation but deficiency of oxygen was increased to the interface of patterned SnO_2/Si substrate where the O/Sn ratio was about 1.73~1.75 at the films. This O deficient state of the film may act as an n-type semiconductor and allow SnO_2 to be applied as a transparent electrode in optoelectronic applications.

Keywords: Tin dioxide, N-type semiconductor, Photochemical metal-organic deposition, XPS depth profiling

1. Introduction

Tin dioxide (SnO_2) has a number of applications as transparent conducting oxides (TCOs) within the fields of electrical devices, displays, and solar cell fabrication in recent years.[1,2] SnO_2 has been actively explored as a promising alternative material to tin-doped indium oxide (ITO; Sn-doped In_2O_3), which has a lot of problems such as high cost due to the rarity of indium, expensive deposition techniques, environmental pollution, and the instability of indium in hydrogen plasma.[3] Because SnO_2, which is an n-type, wide band-gap semiconductor ($E_g = 3.6$ eV), has attracted attention for applications involving transparent electrodes, solar cells, and gas sensors due to non-toxicity, inexpensive cost, highly abundance, and stability in hydrogen plasma compared with ITO.[4]

There have been many reports on the formation of SnO_2 thin films by using chemical vapor deposition (CVD),[5] sputtering,[6] and sol-gel methods.[7] The most common deposition method for SnO_2 thin film is CVD or sputtering, because the dry-deposition process always produces better functional properties of the films than the wet-deposition process. However, the solution deposition technique is simple and inexpensive, as there is no need for expensive target materials or equipment, and it can be easily adapted to accommodate an introduction of additives like metallic nanostructures for an enhancement of electrical property. In this experiment, photochemical metal-organic deposition (PMOD) was used by using photosensitive solution precursors and UV light in order to fabricate the photoresist-free, direct-patterned SnO_2 thin films. We can overcome the disadvantages of dry etching during the fabrication of fine patterns for solid geometric devices through PMOD.

In our previous works, the optical, electrical, and structural properties of direct-patternable SnO_2 films were investigated by annealing the films at various temperatures.[8,9] Normally SnO_2 shows n-type semiconducting characteristic from its oxygen deficient nature. That is to say, SnO_2 could show diverse surface properties depending on the surface composition and chemical state. This is importantly considered when the surface of SnO_2 acts as a main role in the applications, for example, SnO_2 gas sensor. However a compositional analysis for the entire SnO_2 film including the interface with substrate has not yet been systematically studied. Therefore, in this paper, we carried out compositional and chemical bonding state analyses of SnO_2 film on Si

†Corresponding author
E-mail: hhpark@yonsei.ac.kr

substrate using X-ray photoelectron spectroscopy (XPS). With XPS, we can get a composition result together with chemical bonding state information. That is to say, even though the material has multiple oxidation states, it is possible to analyze the qualitative and quantitative chemical bonding state of material including the oxidation state. For the purpose, XPS depth profiling study of PMOD-SnO_2 thin films was accomplished in order to analyze the composition and chemical bonding state of SnO_2 thin film including the interface with Si substrate for usage of direct-patterned SnO_2 thin film to optoelectronic application.

2. Experimental Details

Tin 2-ethylhexanoate, $Sn(O_2CCH(C_2H_5)C_4H_9)_2$, was used as a photosensitive precursor for the production of SnO_2 films. The solvent and sol stabilizer were 4-methyl-2-pentanone and monoethanolamine, respectively. Tin 2-ethylhexanoate was dissolved in 4-methyl-2-pentanone at 0.3 M and monoethanolamine was added for stabilization at a molar ratio of 1.0. The dissolved photosensitive solution was stirred at room temperature for 5 h. The solution was mixed and spin coated on Si substrate using a Fusion 1737 at 2000 rpm for 20 s. For direct patterning of film, the spin-coated film was exposed to UV light (1000 W mercury lamp, λ_{max}=365 nm). Then, the film was washed with 4-methyl-2-pentanone to develop an unexposed area of the film. For crystallization, the direct-patterned thin films were heated at 300°C in a tube furnace under oxygen atmosphere for 10 min, and then the heated films were re-annealed at 600°C in a tube furnace under N_2 atmosphere for 1 h.

The thickness of film was measured using a cross-sectional field emission scanning electron microscopy (FE-SEM; JEOL, JSM 7001F). Crystallinity was analyzed using X-ray diffraction (XRD) beam line 10B at Pohang Light Source (PLS, Pohang, Korea) with $\lambda = 1.5409$ Å and $E = 8.04621$ keV. The images of the direct-patterned films were obtained using an optical microscope. The depth profiling was reported using XPS (Thermo Scientific ESCALAB 250) with an ion beam energy of 3 kV and 2 μA. The sputtering rate was about 19~24 nm per cycle.

3. Results And Discussion

3.1. Fabrication of the direct-patterned SnO_2 thin films

Figure 1 shows (a) optical photograph of direct-patterned SnO_2 thin film after annealing at 600°C for 1 h and (b) the schematic diagram of estimated cross-sectional structure of the sample and the position corresponding to the sputtering

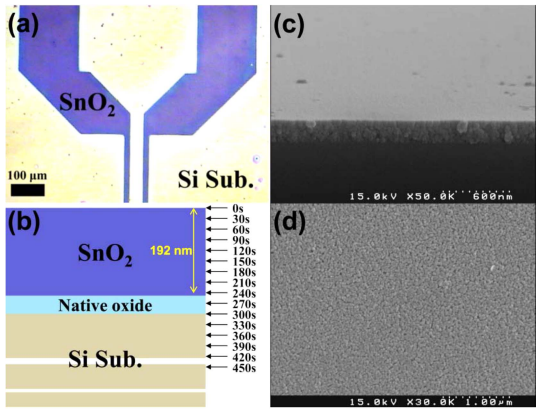

Fig. 1. (a) Optical photograph of the direct-patterned SnO_2 thin film after annealing at 600°C in a N_2 atmosphere for 1 h, (b) the schematic diagram of estimated cross-sectional structure for the sample and the position corresponding to the sputtering time, and the FE-SEM images of (c) cross-section and (d) top-view for SnO_2 thin films.

time. The direct-patterning process was performed by removing the area unexposed to UV light by rinsing with solvent after exposure of the films through a photo mask for 10 min. In Fig. 1(a), the dark area indicates the SnO_2 thin film region and the relatively bright area corresponds to the Si substrate. The line patterned area was well-defined by photoresist-free patterning using PMOD. UV exposure of only 10 min was enough for the fabrication of direct-patterned SnO_2 thin films. Due to the formation of cross-linked network of SnO_2 after exposure to UV light, the exposed region of the film was no longer a fluid state (spin-coated wet state) and then it was not removed by dissolution in successive solvent rinsing step. The (c) cross-sectional and (d) top-view FE-SEM images are also shown in Fig. 1. From the cross-sectional FE-SEM image, the thickness of the SnO_2 film was measured as about 192 nm. The XRD pattern of SnO_2 thin film annealed at 600°C in a nitrogen atmosphere for 1 h was given in Fig. 2. The film exhibited

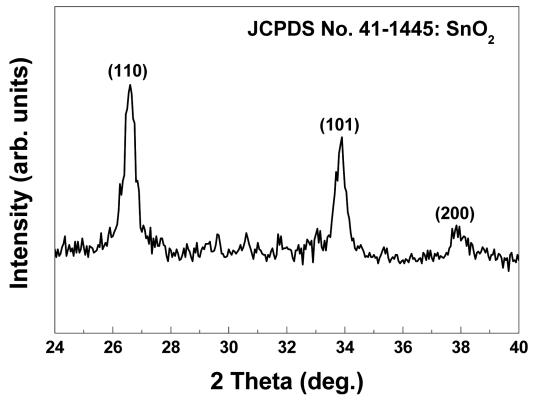

Fig. 2. XRD pattern of direct-patterned SnO_2 thin film after annealing at 600°C in a N_2 atmosphere for 1 h.

the cassiterite phase with tetragonal rutile structure of SnO_2 (JCPDS No. 41-1445) and the grain size of the film was calculated with (110) diffraction peak using the Debye-Scherrer equation. The grain size of the polycrystalline SnO_2 thin film was about 30 nm and this value was well matched with the top-view FE-SEM image in Fig. 1(d).

3.2. XPS depth profiling of SnO_2 films as a function of sputtering time

Figure 3 shows an evolution in time of (a) C 1s and (b) Si 2p photoelectron spectra during subsequent etch time by relative intensity. The time dependent evolution of C 1s peak during sputtering time represents that the C 1s peak indicates only for the un-sputtered surface and it was completely removed after first sputtering cycle (30 s). It was confirmed that carbon does not affect the properties of SnO_2 thin film because the organic ligands were completely decomposed in the SnO_2 thin film after a high temperature annealing step for PMOD process in this work. In the case of Si 2p region, the peak was not visible until the sputtering time for 210 s. Si 2p peaks at 103.3 eV and 99.3 eV are indicated as Si^{2+} bonded with O^{2-} and Si metallic bonding state, respectively.[10] Therefore, it is clearly determined that the interface between SnO_2 and Si substrate exists in the sputtering time ranging from 240 s to 270 s. In this range, the two Si peaks were simultaneously visible because Si-oxide layer was created at the interface between SnO_2 and Si substrate. This layer might be formed by native oxidation and high temperature annealing of SnO_2 thin film. The ion beam sputtering rate per 1 cycle can be estimated by 19 ~ 24 nm, which are calculated by 192 nm-thick-film divided by 8~10 cycles (0 s~240 or 300 s).

Figure 4 provides XPS depth profiling result in (a) Sn 3d and (b) O 1s regions during subsequent etch time by relative intensity. At the surface of SnO_2 thin film (un-sputtered surface), the highest intensity of the Sn $3d_{5/2}$ peak and O 1s peak were observed at the binding energy of 486.8 eV and 530.8 eV, respectively. Those peak positions indicated nearly stoichiometric SnO_2 bonding state even though the peaks may be overlapped to the oxidation states of Sn^{4+}, Sn^{2+}, and Sn^0 in Sn 3d region and O_{Chem} (surface chemisorbed oxygen), O-Sn^{4+}, and O-Sn^{2+} in O 1s region, respectively.[11] After first sputtering time for 30 s, both Sn 3d peak shifted from oxygen rich state to oxygen deficient state (486.3 eV; Sn^{4+} decrease, Sn^{2+} increase) in SnO_2 film (30~210 s) and the O 1s peaks also showed the same behavior related to the Sn^{4+} and Sn^{2+} of Sn $3d_{5/2}$ spectra (peak shifted to 530.2 eV). In the range of sputtering time from 240 s to 300 s, Sn 3d

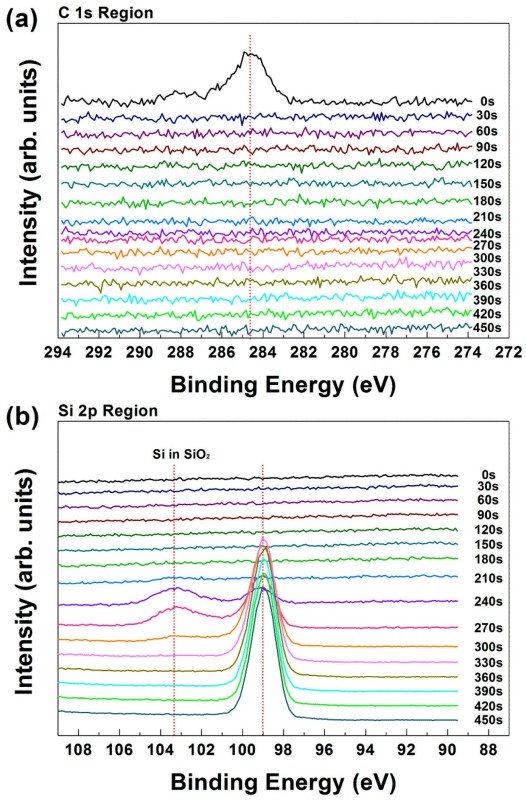

Fig. 3. Evolution of the XPS core level spectra in (a) C 1s region and (b) Si 2p region during subsequent etch time by relative intensity. (Spectra are vertically displaced for clarity)

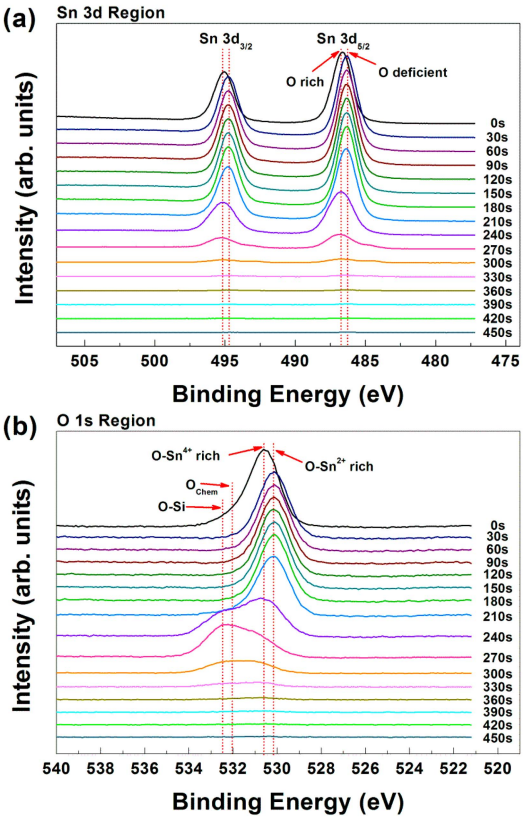

Fig. 4. Evolution of the XPS core level spectra in (a) Sn 3d region and (b) O 1s region during subsequent etch time by relative intensity. (Spectra are vertically displaced for clarity.)

peaks were markedly decreased while O 1s peak in SnO_2 was decreased and O 1s peak corresponding to O-Si^{4+} was increased. This interfacial composition distribution of SnO_2 and Si substrate agreed well with the change of Si 2p peaks in Fig. 3(b).

3.3. Compositional studies for direct-patterned SnO_2 thin films

We investigated the chemical bonding nature of the film and the interface of SnO_2/Si substrate because it can be modified by O-deficiency-related stoichiometry of SnO_2 thin films. This compositional modification along with the depth from the surface can affect the energy-level alignment among the SnO_2 electrode and functional materials in optoelectronic applications. To study the chemical bonding states as a function of depth, surface chemical analysis for the selected sputtering times (0 s, 120 s, and 240 s) was performed. Figure 5 shows the XPS spectra of direct-patterned SnO_2 films in Sn $3d_{5/2}$ and O 1s regions as a function of selected sputtering time. The selected sputtering time was 0 s, 120 s, and 240 s corresponded to the top surface, the film, and also the interface between SnO_2 and Si substrate, respectively. The peak fitting for decomposition of possible bonding states was accomplished by Gaussian line shape fitting with the full width at half maximum (FWHM) of the peaks ranging from 1.2 eV to 1.8 eV. In the case of Sn $3d_{5/2}$ region (Fig. 5(a)), two possible bonding states were decomposed by 486.9 eV and 486.2 eV for all sputtering steps. Two components in Sn $3d_{5/2}$ region are indicated by the Sn^{4+} and Sn^{2+} states and this result was well matched with other reported decomposition result of L-CVD deposited SnO_2 thin films.[12,13] Sn^0 state was not detected in SnO_2 thin films and this suggested that Sn completely bonded with O during the annealing process at high temperature (600ºC). The relative area of Sn^{4+} and Sn^{2+} were 87.3%:12.7%, 64.3%:35.7%, and 76.5%:23.5% for 0 s, 120 s, and 240 s, respectively. As suggested in Fig. 4, the chemical bonding state of Sn^{4+} was dominant at the top surface (0 s) and the interface with substrate (240 s), while Sn^{2+} was relatively increased at 120 s etch time. This result was also reflected by XPS analysis in O 1s region as shown in Fig. 5(b). The O 1s peaks at 532.3 eV, 532.0 eV, 530.6 eV, and 529.8 eV are indicated as the O state bonded with Si, surface chemisorption, Sn^{4+}, and Sn^{2+}, respectively. As similar as the XPS analysis in Sn $3d_{5/2}$ region, O-Sn^{4+} bonding state was dominant at the top surface and the interface area between SnO_2 and Si substrate due to efficient supplement of O into the SnO_2 from the air and native oxide, while O-Sn^{2+} state was relatively high at the film (120 s). This high non-stoichiometric nature inside the film may cause an n-type semiconducting property of SnO_2 thin film through the O deficient nature.

In order to confirm the compositional change of main elements in SnO_2 thin film, the atomic concentration of C 1s, Si 2p, Sn 3d, and O 1s as a function of sputtering time was given in Fig. 6. We finally determined the atomic composition of direct-patterned SnO_2 thin film in-depth. In order to confirm the stoichiometry of SnO_2 thin films as a function of depth, O/Sn ratios were calculated for 0 s, 120 s,

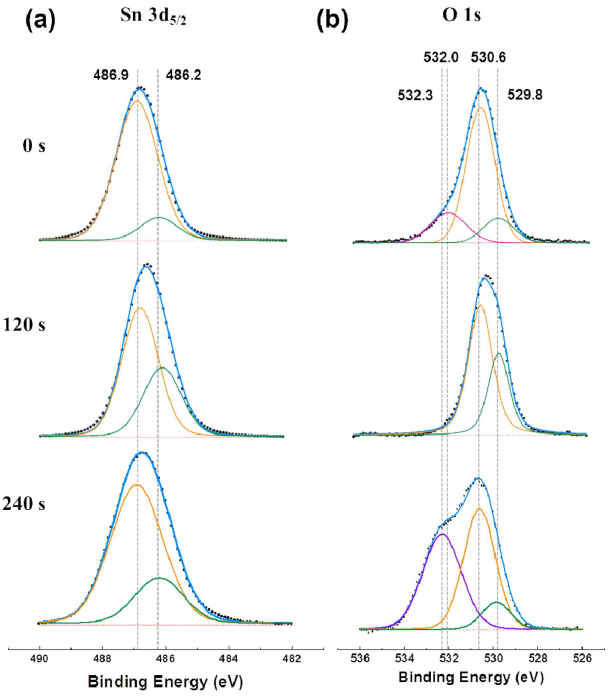

Fig. 5. X-ray photoemission spectra in (a) Sn $3d_{5/2}$ and (b) O 1s region of direct-patterned SnO_2 thin films as a function of sputtering time (0 s; surface of SnO_2 thin film, 120 s; SnO_2 thin film, and 240 s; interface between SnO_2 and Si substrate).

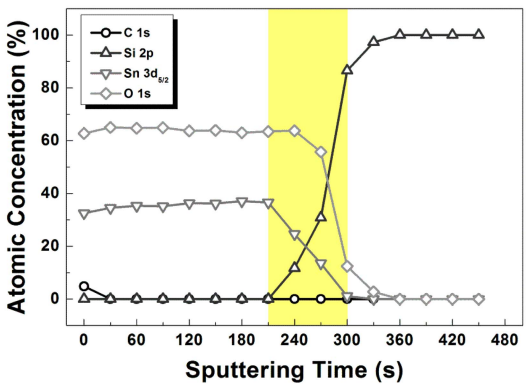

Fig. 6. The atomic concentration of C 1s, Si 2p, Sn 3d, and O 1s as a function of sputtering times. (Yellow square region indicates the interface among SnO_2, native SiO_2, and Si substrate.)

and 210 s. O components could be easily decomposed by O in Sn-oxide or O in Si-oxide, therefore O and Sn atomic ratio could be easily calculated. The calculated values were 1.92, 1.75, and 1.73 for 0 s, 120 s, and 210 s, respectively. This result was well matched with aforementioned bonding states shown in Figs. 4 and 5, and the stoichiometry of SnO_2 thin film almost keeps O deficient composition in photoresist-free patterned SnO_2 thin film except film surface under 24 nm thickness. [11] From the above results, it can be said that the underneath of SnO_2 thin film shows a semiconducting property and it can be served as TCO but there should be a limitation of its usage on chemical sensors and so on due to its full oxidation nature from air oxygen contamination.

4. Conclusions

We successfully fabricated SnO_2 thin films by using direct-pattering process and then analyzed the composition of the films from the top surface of the films to the interface with Si substrate. Even though the interface boundary could not be determined accurately because the SnO_2, SiO_2, and Si substrate are mixed in the range of sputtering time from 210 s to 300 s, the chemical bonding states at the three main regions and Sn/O stoichiometric ratio could be analyzed in direct-patterned SnO_2 thin films as oxygen-deficient. This depth profiling information provides the chemical bonding states of SnO_2 thin films from the surface to the interface between coated, functional material and substrate as a function of depth. In case of SnO_2, it shows semiconducting property due to its oxygen-deficient characteristic but after exposure to air, a fully oxidizing state of SnO_2 was formed at the surface. From this surface oxidation behavior, there should be a limitation of SnO_2 for surface sensing application.

Acknowledgements

This work was supported by the Industrial Strategic technology development program (10041926, Development of high density plasma technologies for thin film deposition of nanoscale semiconductor and flexible display processing) funded by the Ministry of Knowledge Economy (MKE, Korea). Experiments at PLS were supported in part by MEST and POSTECH.

References

1. W. Zhang, R. Zhu, X. Liu, B. Liu and S. Ramakrishna, “Facile construction of nanofibrous ZnO photoelectrode for dye-sensitized solar cell applications”, Appl. Phys. Lett. 95, 043304 (2009).
2. H. K. Kim and R. Y. Lee, “NO_2 gas sensing properties of SnO_2 thin films dopped with Pd and CNT”, J. Microelectron. Packag. Soc., 15(4), 101 (2008).
3. J. H. Yoo and H. J. Chang, “Preparation of polymer light emitting diodes with PFO-poss organic emission layer on ITO/glass substrates”, J. Microelectron. Packag. Soc., 13(4), 51 (2006).
4. J. F. Wager, D. A. Keszler and R. E. Presley, “Transparent Electronics”, Springer, USA (2008).
5. D. J. Houlton, A. C. Jones, P. W. Haycock, E. W. Williams, J. Bull and G. W. Critchlow, “The deposition of platinum-containing tin oxide thin films by metal-organic CVD”, Chem. Vap. Deposition, 1, 26 (1995).
6. S. H. Kim, K. T. Lee, J. H. Moon and B.-T. Lee, “Effects of Pt/Pd codoping on the sensitivity of SnO_2 thin film sensors”, Jpn. J. Appl. Phys. 41, L1002 (2002).
7. M. D’Arienzo, L. Armelao, A. Cacciamani, C. M. Mari, S. Polizzi, R. Ruffo, R. Scotti, A. Testino, L. Wahba and F. Morazzoni, “Onestep preparation of SnO_2 and Pt-doped SnO_2 as inverse opal thin films for gas sensing”, Chem. Mater., 22, 4083 (2010).
8. Y.-J. Choi, H.-H. Park, S. Golledge, D. C. Johnson, H. J. Chang and H. Jeon, “The electrical and optical properties of direct-patternable SnO_2 thin films containing Pt nanoparticles at various annealing temperatures”, Surf. Coat. Technol., 205, 2649 (2010).
9. Y.-J. Choi and H.-H. Park, “Direct patterning of SnO_2 composite films prepared with various contents of Pt nanoparticles by photochemical metal-organic deposition”, Thin Solid Films, 519, 6214 (2011).
10. M. R. Alexander, R. D. Short, F. R. Jones, W. Michaeli and C. J. Blomfield, “A study of HMDSO/O_2 plasma deposits using a high-sensitivity and –energy resolution XPS instrument: curve fitting of the Si 2p core level”, Appl. Surf. Sci., 137, 179 (1999).
11. S. G. Ansari, M. A. Dar, M. S. Dhage, Y. S. Kim, Z. A. Ansari, A. Al-Hajry, H.-S. Shin, “A novel method for preparing stoichiometric SnO_2 thin films at low temperature”, Rev. Sci. Instrum. 80, 045112 (2009).
12. M. Kwoka, L. Ottaviano, M. Passacantando, S. Santucci, G. Czempik, J. Szuber, “XPS study of the surface chemistry of L-CVD SnO_2 thin films after oxidation”, Thin Solid Films, 490, 36 (2005).
13. M. Kwoka, L. Ottaviano, M. Passacantando, S. Santucci, J. Szuber, “XPS depth profiling studies of L-CVD SnO_2 thin films”, Appl. Sur. Sci., 252, 7730 (2006).